**Modeling the Q-CTRL Cloud Qubit**

**A. Anakru, J. Crossman, C. Gerlach, and C. Schwarze**

**Synopsis**

In Section I, we outline our strategy for reverse engineering several aspects of the Q-CTRL simulated cloud qubit. In Section II, we show how these findings are incorporated into a model Hamiltonian and ultimately are used to construct quantum gates.

# 1 System Identification

## Decoherence, Population Decay, and Upper State Excitations

The initial state is approximately $|0\rangle$, and we plot $|\langle 0|\psi(T)\rangle|^2$ for durations $T \in [0, 300]$, one for each of the 100 controls. In each case, the value array is a flat 1.0 throughout the duration, corresponding to maximum Rabi frequency. Each point is the average of 1024 independent shots.

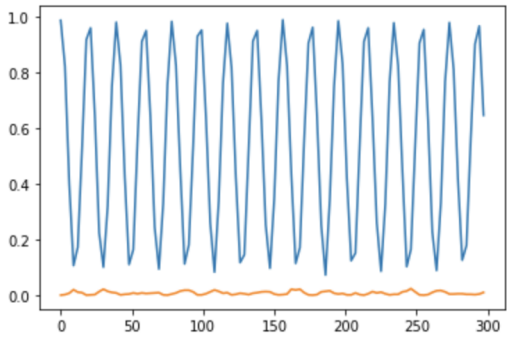


Figure 1: Blue: $|\langle 0|\psi(T)\rangle|^2$ vs duration $T$. Orange: $|\langle 2|\psi(T)\rangle|^2$ vs duration $T$

Here we see many full Rabi oscillations without any noticeable decay. We thus conclude that the effects of population decay and decoherence are negligible on the timescales that we are interested in. We also see that the 2nd excited state $|2\rangle$ consistently has very small occupation probability, so to very good approximation, we may neglect it and treat our two lowest levels as a closed quantum system (lossless qubit).

## System Preparation and Measurement (SPAM)

Simulations were preformed on the cloud qubit to estimate the SPAM error rate. A pulse of negligible duration was fed to the system for $3,072,000$ individual shots, and the final states were measured. For such a short pulse, the probability of observing the system in $|1\rangle$ was assumed to be very small, and so the SPAM probability was taken to be the ratio of $|1\rangle$ observations to the total number of trials. Thus, we found the SPAM-averaged population of the first excited state to be $\langle|\langle 1|\Psi(t=0)\rangle|^2\rangle_{noise} = 0.01005305989 \approx 1\%$, where the square brackets indicate averaging over noise and error. We assumed the SPAM error rate was symmetric, that is, preparation error was equal to measurement error, for no test could be devised to estimate the latter.

This suggests that the infidelity metric to use for a single NOT gate (assuming we start from the above initial ensemble of states affected by state-preparation error) is

$$f = 1 - \langle|\langle 1|\Psi(t=0)\rangle|^2\rangle_{SPAM} - \langle|\langle 1|\Psi(t=T)\rangle|^2\rangle_{noise}$$

where $|\Psi(t=T)\rangle$ represents the state right after we apply the NOT gate, and $f = 0$ would imply perfect fidelity.

## Rabi Frequency Calibration

A series of cloud-qubit simulations were conducted with a range of so-called value parameters, and nonlinear curve fitting was used to measure the corresponding Bloch sphere frequency. From the following formula, one can extract

both the Rabi frequency $\Omega_R$ and the detuning (dephasing) $\Delta$ from the empirical measurements of the Bloch sphere frequency $\Omega$:

$$\Omega^2 = \Omega_R^2 + \frac{\Delta^2}{\hbar^2} \tag{1}$$

Indeed, for large values of $\Omega_R$, we have $\Omega \approx \Omega_R$ to very good approximation, and similarly, for small values of $\Omega_R$, $\hbar\Omega \approx \Delta$. In each regime, a linear fit was applied to the relationship between the normalized pulse amplitude value and the measured $\Omega$. From this we extracted the model parameters $\Omega_R$ and $\Delta/\hbar$. We deduced that the dominant effect to model was that of detuning (dephasing).

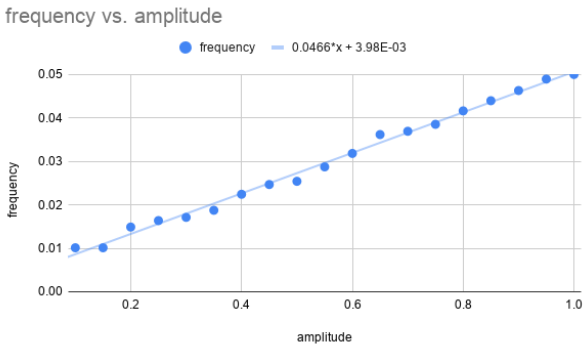


Figure 2: Blue: Frequency vs Amplitude for large amplitude. This data was used to extract the maximum Rabi frequency $\Omega_R$ and its relationship to the 'value' input levels.

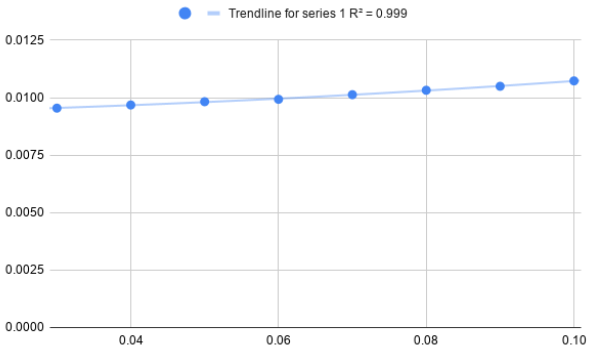


Figure 3: Blue: Frequency vs Amplitude for small amplitude. This data was used to extract the detuning $\Delta$.

## 2 Determining Input Pulses for the Cloud Qubit

With the Rabi rate $|\Omega_R|^2$ and the detuning $\Delta/\hbar$, we can write a model Hamiltonian:

$$\frac{1}{\hbar}H_{model} = \frac{\Delta}{2}\sigma_z + \frac{\Omega_R(t)}{2}\sigma_- + \frac{\Omega_R^*(t)}{2}\sigma_+$$

Since the Rabi rate calculation cannot determine the phase of $\Omega_R(t)$ (nor the sign of $\Delta$), we assume both of these parameters are nonnegative real numbers. Having established a simple, constant-detuning centered model with the findings in the previous section, we now turn to studying this system in detail. While an overly simplified model might be regarded as too idealistic, we shall soon see the theoretical advantages such a model permits.

Let our basis of states be $|0\rangle, |1\rangle$; given any normalized pure state $|\psi(t)\rangle$, we can write a density operator $\rho(t) = |\psi(t)\rangle\langle\psi(t)|$, where the matrix elements are denoted $\rho_{ij}$ $(i,j \in \{1,2\})$. Then it can be shown that when we define $V_x = 2\mathrm{Re}(\rho_{12}), V_y = 2\mathrm{Im}(\rho_{12}), V_z = \rho_{22} - \rho_{11}$, the vector $\vec{V}(t)$ obeys

$$\frac{d\vec{V}}{dt} = \vec{\Omega}(t) \times \vec{V}$$

where $\vec{\Omega} = -\Omega_R(t)\hat{x} + \Delta\hat{z}$. Thus, we can visualize the effects of unitary transformations (controlled by $\Omega_R(t)$) as rotations on the 'Bloch Sphere'. All frequencies are measured in megahertz.

## 2.1 Constructing a NOT gate: Theory

In the absence of detuning, fixing $\Omega_R(t) = \Omega_{R0}$ for a duration $0 \le t \le \Omega_{R0}^{-1}$ is sufficient to act as a NOT gate (i.e. it flips $|0\rangle$ to $|1\rangle$ and vice versa). However, the situation is more complicated in the presence of detuning. We have developed a theoretical amplitude profile $\Omega_R(t)$ designed to yield a high-fidelity NOT gate even with detuning (so long as the detuning is measured precisely). Specifically, we have

$$\Omega_R(t) = \begin{cases} \Omega_{R0} & 0 \le t \le T_1 \\ 0 & T_1 \le t \le T_1 + T_2 \\ \Omega_{R0} & T_1 + T_2 \le t \le T_1 + T_2 + T_3 \end{cases}$$

$$T_1 = \frac{1}{2\pi}\frac{1}{\sqrt{\Omega_{R0}^2 + \Delta^2}}\arccos\left(-\frac{\Delta^2}{\Omega_{R0}^2}\right); \quad T_2 = \frac{0.5}{\Delta}; \quad T_3 = \left(\frac{1}{\sqrt{\Omega_{R0}^2 + \Delta^2}} - T_1\right)$$

On the Bloch sphere, applying a NOT gate must flip $\vec{V}_{\text{initial}} = -\hat{z}$ to $\vec{V}_{\text{final}} = +\hat{z}$, and vice versa. The above form of $\Omega_R(t)$ accomplishes this (with $\Omega_{R0} = 48.615$ kHz) by first rotating $\vec{V}$ into the $y - z$ plane, then turning the Rabi rate off, letting the $\vec{V}$ rotate (under detuning alone) by an angle of $\pi$ (which effectively flips the sign of $\vec{V}$), then turn the Rabi rate back on during the third time interval to invert the rotation induced by the first $T_1$ duration of the pulse. Thus a pulse of this form for the given duration $T = T_1 + T_2 + T_3$ constitutes an 'ideal' NOT gate, assuming this Hamiltonian model is accurate.

## 2.2 Implementing and Optimizing the NOT Gate

In our system, we had measured $\Delta = 9.29671$ kHz and the maximum Rabi rate to be $\Omega_{R0} = 48.615$ kHz, leading to theoretical values of $T_1 = 5.235$ $\mu$s, $T_2 = 53.782$ $\mu$s, $T_3 = 15.218$ $\mu$s. We discretized this pulse (while remaining as faithful as possible to the total duration and the ratios $T_3/T_1, T_2/T_1$) with 223 segments. After optimizing over the total pulse duration to correct for errors (that could come from measurement of the Hamiltonian parameters, the discretization of our theoretical ideal pulse, etc.) and modifying the infidelity function to account for our SPAM noise, we measure a fidelity of $-4.32 \times 10^{-3}$ over 100,000 shots.

## 2.3 Constructing a Hadamard gate: Theory

We may make similar use of Bloch Sphere Dynamics to construct a pulse that implements a Hadamard gate:

$$\Omega_R(t) = \begin{cases} \Omega_{R0} & 0 \le t \le T_1 \\ 0 & T_1 \le t \le T_1 + T_2 \end{cases}$$

and $T_1$ and $T_2$ are the same as in the previous section. The first part of the pulse (up to $T_1$) rotates $\vec{V}$ into the y-x plane, and the second part of the 'pulse' (where the field is just turned off) rotates the vector by $\pi$ radians about the $\hat{z}$ axis; this second step is necessary to ensure $\hat{H}_g^2 = 1$ on our qubit, where $\hat{H}_g$ is the Hadamard operator matrix.

## 2.4 Implementing and Optimizing the Hadamard Gate

Implementation of this pulse proceeds similarly as with the NOT gate; we discretized this pulse with 225 segments. After optimizing over the total pulse duration and accounting for SPAM, we measure a fidelity of $1.833 \times 10^{-2}$.

## Appendix: Source Listing

`https://courses.cit.cornell.edu/ece531/Lectures/Lectures.htm`
`https://docs.q-ctrl.com/boulder-opal/application-notes/q-ctrl-qchack-challenge`